Biogeosciences Discuss., 10, 5749–5780, 2013
www.biogeosciences-discuss.net/10/5749/2013/
doi:10.5194/bgd-10-5749-2013

Biogeosciences
Discussions
Open Access

Modeling microbial exchanges between forms of soil nitrogen in contrasting ecosystems

M. Pansu[1], **D. Machado**[2], **P. Bottner**[3], **and L. Sarmiento**[4]

[1]IRD, UMR Eco&Sol (Supagro, Cirad, Inra, IRD), Place Viala, Montpellier, France
[2]Laboratorio de Investigación en Análisis Químico Industrial y Agropecuario, Departamento de Química, Facultad de Ciencias, Universidad de los Andes, Mérida, Venezuela
[3]CEFE-CNRS Deceased 15 October 2006, Montpellier, France
[4]Instituto de Ciencias Ambientales y Ecológicas, Facultad de Ciencias, Universidad de los Andes, Merida, Venezuela

Received: 16 January 2013 – Accepted: 8 March 2013 – Published: 25 March 2013

Correspondence to: M. Pansu (marc.pansu@ird.fr)

Published by Copernicus Publications on behalf of the European Geosciences Union.

Abstract

Although nitrogen (N) is often linked to carbon (C) in organic molecules, C is carried from the atmosphere to the soil through plants while N is carried from the soil to plants by microbial transformations. Many schemes have been proposed to describe the microbial conversion between organic and inorganic forms of N but current models do not fully represent the microbial control over these conversions. This study followed the transfer of ^{15}N between plant materials, microorganisms, humified compartments and inorganic forms in 6 very different ecosystems along an altitudinal transect. The microbial conversion of the ^{15}N forms appeared to be strongly linked to that found previously for ^{14}C forms since the parameters and relationships defined for C were appropriate for modeling the N cycle. The only difference was in the flows between microbial and inorganic forms. The CO_2-C loss was modeled using the equation for microbial respiration. Inorganic N appears also closely associated with microorganisms, which, depending on their C : N ratio and those of the available substrates, regulate the N mineralization and immobilization processes. Applications at earth scale can use the approximation that the microbial C : N ratio does not vary with time, but for this study, microorganisms cannot be treated always as homeostatic as their C : N ratio can decrease during incubation and increase with altitude when C storage increases. The MOMOS model has been validated for the C cycle, and it also appears to be valid for microbial conversion of N forms. It uses a relatively small number of well-defined, climate-dependent parameters, and it should fill a gap in the range of current models based on a direct microbial control for describing C and N flows in ecosystems.

1 Introduction

Nitrogen (N) in living plants represents about 5 % of the global N stock: it is adsorbed by plant roots mostly in mineral forms in small quantities in soil, where more than 90 % of N is in organic form (Lin et al., 2000; Pansu and Gautheyrou, 2006). Microbial exchanges play a major role in the N cycle that must be considered in conjunction with the carbon (C) cycle. Mechanistic models are required to give an accurate prediction of all the transfers of N between organic and inorganic compartments of various stabilities. Manzoni and Porporato (2009) classified the published N models as SIMP for simplified formulations, MIT for mineralization/immobilization turnover mechanisms which assume a transfer of organic to inorganic N pools before microbial assimilation, DIR for direct microbial assimilation of all available organic N, MIX for models combining DIR and MIT principles and PAR for a parallel DIR/MIT scheme including direct assimilation, ammonium production by microorganisms and then microbial assimilation of the ammonium produced (Barraclough, 1997). With increasing knowledge of the mechanisms, the types of models available have changed from 60 % SIMP and 40 % MIT in 1970 to 5 % SIMP, 7 % MIT, 5 % MIX, 17 % PAR, and 66 % DIR in 2010.

Organic N transformations have often been modeled by considering compartments with different C : N ratios (e.g. van Veen and Ladd, 1985; Bradbury et al., 1993; Carter et al., 1993; Dou and Fox, 1995; Quemada and Cabrera, 1995; Richter and Benbi, 1996; Franko, 1996; Mueller et al., 1998; Garnier et al., 2001; Nicolardot et al., 2001; Pansu et al., 2003, 2004; Neill and Gignoux, 2006), but Todd-Brown et al. (2012) considered that "current global models do not represent direct microbial control over decomposition" and a new generation of models is required. An important aspect is related to the stoichiometry of decomposers (Sterner and Elser, 2002). Microbial biomass (MB) has often been considered homeostatic, i.e. with a composition independent of that of the substrates used, implying that assumptions are made to maintain a constant MB C : N ratio, but other models and experimental data (Bottner et al., 2006) allow the C : N ratio of MB to change with time in response to the substrate C : N ratio and changes in the microbial communities during decomposition.

This work deals with N dynamics along an altitudinal transect previously used to validate the MOMOS-C model (Pansu et al., 2010). The aim was to predict the conversion of the ^{15}N labeled forms simultaneously with the conversion of ^{14}C labeled forms, assuming that MB can assimilate some N from labile and stable molecules of plant

and microbial origin as well as some N from the soil inorganic N pool (see above PAR scheme). This raised three questions:

1 Can it be considered that microbial enzymatic assimilation rates are the same for C and N?

2 Can it be considered that C transfers by microbial respiration and mortality cause simultaneous transfers of N into labile humus and inorganic forms to balance the MB C : N ratio? Can the assimilation of inorganic N be modeled to sustain microbial activity in the case of an N deficit during conversion of organic forms?

3 Can it be considered that the microbial biomass is homeostatic or does it have a C : N ratio that varies through incubation periods and is different in ecosystems at different altitudes?

2 Materials and methods

2.1 The experimental sites

The experiment was carried out in six sites (Table 1) along an altitudinal transect in Venezuela, from 65 to 3968 m a.s.l., covering a large bioclimatic gradient that comprised tropical rainforest (A(65)), natural savanna (A(165)), seasonal montane forest (A(780)), cloud forest (A(1800)) and Andean páramo (alpine vegetation) at two heights (A(3400) and A(3968)). The sites have been described in previous publications (Couteaux et al., 2002; Pansu et al., 2010). This altitudinal transect is characterized by contrasting conditions of temperature, annual precipitation and its seasonal distribution, and soil characteristics. The long-term mean annual air temperature ranged from 5.5 °C at A(3968) to 27.4 °C at A(65), the mean annual precipitation ranged from 790 mm at A(3968) to 1992 mm at A(1800). Soils were acid in all sites but particularly in the two páramo soils. The soils were loam at A(3400) and sandy loams at the other sites. The savanna soil at site A(165) contained the highest amount of sand and the lowest amount of organic matter, both water holding capacity (WHC) and cation exchange capacity (CEC) were lower than any of the other sites. The mountain soils A(1800) and A(3400) contained the highest amounts of fine particles and organic matter and had the highest WHC and CEC. The three other soils had intermediate WHC and CEC. The carbon content in the 0–10 cm soil layer varied from 13 g (C) kg^{-1} at A(165) to more than 100 g (C) kg^{-1} (soil) at A(1800) and A(3400). The quality of the soil organic matter was also variable, with C : N ratios ranging from 13 at A(65) and A(780) through 15 at A(165) up to 17 to 22 at the highest sites A(1800) to A(3968).

2.2 Experimental design and data collection

Plots with herbaceous vegetation were selected at each site to minimize the variability due to the effect of soil cover on microclimate conditions, mainly on soil temperature. For the savanna and alpine ecosystems, areas with natural vegetation were selected, but for the forest ecosystems, plots on managed grassland were selected. ^{14}C and ^{15}N labeled straw was mixed with soil, from the top 0–10 cm layer at each of the sites, in 14 × 15 cm porous bags. The top part of the bags had a 1 mm mesh to allow the passage of plant roots and mesofauna and the mesh of the bottom part was 0.1 mm to minimize losses by gravity. The soil weight per bag was adjusted to reproduce the natural bulk density for a volume of 210 cm^3. The labeled straw was obtained by growing the wheat in a labeling chamber with controlled temperature, radiation, humidity and CO_2 concentration. The wheat was grown from seed to maturity in four months in a ^{14}C labeled atmosphere with a ^{15}N labeled, NPK + micro-nutrient solution. The straw, containing 392 mg C g^{-1} and 12.33 mg N g^{-1} (C : N ratio of 31.79), was roughly ground to < 5 mm particles. The N and ^{15}N composition of the soil in the bags is given in Table 2. The added carbon and nitrogen from the straw ranged from 1.2 % (A(3400)) to 13.8 % (A(165)) of the native C and 0.70 % (A(3400)) to 6.60 % (A(165)) of the native N in the soil.

40 bags containing the labeled straw and soil were buried 5 cm deep along four parallel lines in each experimental plot (10 samples at different times × 4 replicates for each sample at each site, making a total of 240 soil bags). When the plots were set

up (23 November to 6 December 1994), the soil bags were moistened with de-ionized water to the midpoint between WHC and the water content at wilting point (WCWP) (Table 1). On each sampling date, one bag from each line of the four lines at each site was selected at random to measure soil water content, total ^{14}C and ^{15}N and ^{14}C and ^{15}N in the microbial biomass and inorganic N stock. The soil bags were left in the soil for 18 months at the two lowest sites (A(65) and A(165)) 24 months at A(780), 31 months at A(1800) and 38 months at the two highest sites (A(3400) and A(3968)). The first samples were taken one month after setting up the experiment and the sampling interval increased with time to 6 months at the end of the experiment for the highest sites. After collection, the soil bags were stored refrigerated for no more than three days before analysis.

Total N was determined by Kjeldahl digestion by boiling in concentrated sulfuric acid with a potassium sulfate-copper sulfate-grey selenium catalyst for 2 h at 400 °C. The ammonia in the solution was then distilled with sodium hydroxide into a standard H_2SO_4 solution and the excess H_2SO_4 was determined by back titration with an NaOH standard solution. After titration, the distillate was acidified to pH between 3 and 4 to avoid N losses and evaporated to obtain ammonium sulfate crystals that were analyzed for ^{15}N abundance using mass spectrometry.

The MB N was determined by fumigation-extraction (Brookes, 1985). After homogenization, a fresh soil sample equivalent to 30 g dry soil was fumigated with alcohol free chloroform for 18 h. The fumigated sample and an equivalent control soil sample were treated with 150 mL of 0.5 mol (K_2SO_4) L^{-1} solution for 30 min and centrifuged. The extracts were digested, titrated, crystallized and analyzed for ^{15}N as for total N. The N labeled part of the microbial biomass was calculated as the difference between the labeled N in the fumigated and control samples, corrected by a K_N factor of 0.54 (Joergensen and Mueller, 1996). An aliquot of the extracted solution from the unfumigated samples was used to determine the total inorganic N and ^{15}N abundance (ammonium and nitrate separately).

For all compartments (total soil, microbial biomass and mineral nitrogen) the percentage of the N in the samples that had come from the N added in the straw (%Ndff) was calculated as:

$$\%\text{Ndff} = \frac{\%E_{\text{comp}}}{\%E_{\text{straw}}} \cdot 100$$

where $\%E_{\text{comp}}$ is the atom percent excess of the tracer in the compartment and $\%E_{\text{straw}}$ is the atom percent excess in the straw. From this, the amount of N from the straw in each compartment was calculated as:

$$\text{mg N} = \frac{\%\text{Ndff} \cdot \text{N}_{\text{total}}}{100}$$

where N_{total} is the total N in the sample in mg.

Following the death of our colleague, Pierre Bottner, we recovered most of the experimental data, except the last results for BM and inorganic ^{15}N, where only the first five results were available for each site.

All ^{15}N labeled data and ^{14}C labeled data (Pansu et al., 2010) are expressed as a fraction of the labeled N and C added at the start of the experiment. As the labeled inorganic N in the soil bags was very low compared to the total labeled ^{15}N, the total labeled ^{15}N was considered to be the labeled organic ^{15}N, the difference between the ^{15}N added in the straw and the organic ^{15}N being the production of inorganic ^{15}N which was assumed to have been lost mostly by root uptake, leaching and gaseous losses through the porous soil bags.

The soil water content was measured in each soil bag using four 5 g replicates that were dried at 105 °C for 24 h. Other soil analyses were performed using standard methods (Pansu and Gautheyrou, 2006).

2.3 The decomposition model MOMOS

As carbon and nitrogen are closely associated in living organisms, it was assumed that the nitrogen cycle could be modeled in MOMOS-N in the same way as the carbon

cycle in MOMOS-C (Pansu et al., 2004, 2010), using the subscript e (either C or N) to differentiate each element in the model.

MOMOS (Fig. 1) was defined as a five compartment model centered on the activity of soil microbial biomass (MBe) that grows by assimilation of labile (VLe) and stable (VSe) fractions of plant necromass (NC) as well as labile (HLe) and stable (HSe) fractions of humus. The microbial mortality regulates humus formation. The only process which is considered more of a chemical process than a biological process is humus stabilization from HLe to HSe. The only difference between the C and N models is in the outputs from MBe to inorganic forms of C (CO_2-C) and N (NH_4-N) or possibly inputs from inorganic N into MB_N. MOMOS has only seven first order kinetic parameters (dimension day^{-1}) and does not need the partitioning coefficients used in other decomposition models. Using the assumption that enzymatic assimilation rates from organic matter, are the same for C and N (see question 1 in the introduction), the best fit parameter values previously found for the C cycle are all used to describe the N cycle for each of the 6 ecosystems (Table 3). All the C and N parameters are conditioned by functions of the soil temperature and water content ranging from 0 to 1, as in the general MOMOS equation:

$$\dot{\boldsymbol{x}}_{\mathbf{e}} = f(T)f(\theta)\mathbf{A}_{\mathbf{e}}\boldsymbol{x}_{\mathbf{e}} + \boldsymbol{B}_{\mathbf{e}} \tag{1}$$

where $\boldsymbol{x}_{\mathbf{e}}$ is the vector of the state variables (^{14}C or ^{15}N content of the compartments), $\dot{\boldsymbol{x}}_e$ is the vector of the derivatives of $\boldsymbol{x}_{\mathbf{e}}$, $\mathbf{A}_{\mathbf{e}}$ is the model parameter matrix for each organic element, $\boldsymbol{B}_{\mathbf{e}}$ is a vector determining the external C and N inputs (see Pansu et al., 2009 for C inputs from living roots, $\boldsymbol{B}_{\mathbf{e}} = 0$ for ^{14}C and ^{15}N labeled data in this experiment) and $f(T)$ is an exponential function of temperature (Pansu et al., 2010):

$$f(T) = Q_{10}^{(T-T_{\text{opt}})/10} \tag{2}$$

where T is the actual daily temperature of soil (0–10 cm layer) set equal to the air temperature; T_{opt} is the optimum decomposition temperature set to 28 °C, a temperature often used to perform laboratory experiments under optimum conditions (Thuriès et al., 2002) and just above the mean annual temperature of the warmer sites A(65) and A(165) of this study; Q_{10} is the factor by which the rate increases with a 10 °C increase in temperature. This was set to 2.2 for all sites for this study (see discussion in Pansu et al., 2010); $f(\theta)$ is the response function to soil moisture expressed as a fraction of the WHC (Table 1, see discussion in Pansu et al., 2010):

$$f(\theta) = \mathrm{MIN}\left(\frac{\theta}{\mathrm{WHC}}, 1\right) \tag{3}$$

The soil water content θ was predicted using the SAHEL model (Penning de Vries et al., 1989). This model calculates the daily water content for each soil layer using meteorological data (daily minimum and maximum temperature, precipitation and latitude), WHC (Table 1) and plant cover as inputs. SAHEL was calibrated for each site using the water content of the soil in the soil bags and then daily water content values for the 0–10 cm layer were generated (Pansu et al., 2004). Meteorological data for the period over which the experiment was carried out was collected for each site from the nearest weather station or estimated using local or archive data, a transition probability matrix and climate corrections as described in Pansu et al. (2010)

The model matrices $\mathbf{A_C}$ and $\mathbf{A_N}$ are:

$$\mathbf{A_C} = \begin{bmatrix} -k_{\mathrm{VL}} & 0 & 0 & 0 & 0 \\ 0 & -k_{\mathrm{VS}} & 0 & 0 & 0 \\ k_{\mathrm{VL}} & k_{\mathrm{V}S} & -\left(q_{\mathrm{CO_2}} + k_{\mathrm{MB}}\right) & k_{\mathrm{HL}} & k_{\mathrm{HS}} \\ 0 & 0 & k_{\mathrm{MB}} & -(k_{\mathrm{HL}} + k_{\mathrm{HLS}}) & 0 \\ 0 & 0 & 0 & k_{\mathrm{HLS}} & -k_{\mathrm{HS}} \end{bmatrix} \text{ and}$$

$$\mathbf{A_N} = \begin{bmatrix} -k_{\mathrm{VL}} & 0 & 0 & 0 & 0 \\ 0 & -k_{\mathrm{VS}} & 0 & 0 & 0 \\ k_{\mathrm{VL}} & k_{\mathrm{VS}} & -\left(f(x_{\mathrm{C,MB}}x_{\mathrm{N,MB}})/f(T)f(\theta)x_{\mathrm{N,MB}} + k_{\mathrm{MB}}\right) & k_{\mathrm{HL}} & k_{\mathrm{HS}} \\ 0 & 0 & k_{\mathrm{MB}} & -(k_{\mathrm{HL}} + k_{\mathrm{HLS}}) & 0 \\ 0 & 0 & 0 & k_{\mathrm{HLS}} & -k_{\mathrm{HS}} \end{bmatrix}$$

The vectors $\boldsymbol{x}_{\mathbf{C}}$ and $\boldsymbol{x}_{\mathbf{N}}$ of the C and N concentrations in each compartment are:

$$\boldsymbol{x}_{\mathbf{C}} = \begin{bmatrix} x_{\mathrm{C,VL}} \\ x_{\mathrm{C,VS}} \\ x_{\mathrm{C,MB}} \\ x_{\mathrm{C,HL}} \\ x_{\mathrm{C,HS}} \end{bmatrix} \qquad \boldsymbol{x}_{\mathbf{N}} = \begin{bmatrix} x_{\mathrm{N,VL}} \\ x_{\mathrm{N,VS}} \\ x_{\mathrm{N,MB}} \\ x_{\mathrm{N,HL}} \\ x_{\mathrm{N,HS}} \end{bmatrix} \tag{4}$$

and the C : N ratios of each compartment are: $C : N_i = \frac{x_{\mathrm{C},i}}{x_{\mathrm{N},i}}$.

For each incubation period, the derivative of C is[1]:

$$\dot{\mathrm{C}} = \sum_{i=1}^{5} \dot{x}_{i,\mathrm{C}} = -f(T)f(\theta)q_{\mathrm{CO_2}}x_{\mathrm{C,MB}} \tag{5}$$

where $q_{\mathrm{CO_2}}$ is the metabolic quotient of the microbial biomass:

$$q_{\mathrm{CO_2}} = k_{\mathrm{resp}}\frac{x_{\mathrm{MB}}}{C^0_{\mathrm{MB}}} \tag{6}$$

where k_{resp} is the respiration coefficient, (dimension day^{-1}) scaled by C^0_{MB}, the biomass at steady state (estimated on untreated soil without recent addition of substrate. In this case, it was estimated from the values of MB-^{14}C measured at the end of incubation).

For each incubation period, the derivative of the total organic N is the negative of the derivative of total inorganic N and is expressed by:

$$\dot{\mathrm{N}} = \sum_{i=1}^{5} \dot{x}_{i,\mathrm{N}} = -f(x_{\mathrm{C,MB}}, x_{\mathrm{N,MB}}) \tag{7}$$

---

[1] The Eq. (5) previously given for MOMOS-C (Pansu et al., 2010) had an optimum $\dot{\mathrm{C}}$ which must be multiplied by $f(T)f(\theta)$ to give a $\dot{\mathrm{C}}$ adjusted for weather conditions. $q\mathrm{CO_2}$ on the right-hand scale of Fig. 3c–8c of Pansu et al. (2010) must be changed to $f(T)f(\theta)q\mathrm{CO2}$.

where positive values of the function $f(x_{\mathrm{C,MB}}, x_{\mathrm{N,MB}})$ correspond to N mineralization of microbial N and negative values correspond to microbial immobilization of inorganic N.

As the simulation concerned only the ^{14}C and ^{15}N introduced in the straw, the initial conditions for C and N compartments of microbial origin were set to zero. If C_0 is the amount of added ^{14}C (= 1 for these data scaled by the ^{14}C input) and f_S is its stable fraction, the initial conditions for the ^{14}C simulation were given by:

$$x_{\mathrm{C,VL}}(0) = (1 - f_S)C_0, x_{\mathrm{C,VS}}(0) = f_S C_0, x_{\mathrm{C,MB}}(0) = x_{\mathrm{C,HL}}(0) = x_{\mathrm{C,HS}}(0) = 0 \tag{8}$$

The stable fraction f_S was estimated as that of the stable compartment of the TAO (Transformation of Added Organic materials) model (Thuriès et al., 2002) between f_S and biochemical composition of straw, which gave $f_S = 0.14$. If η_{NC} is the C : N ratio of labeled NC, and η_{VS} the C : N ratio of the stable fraction of NC, the initial conditions for the ^{15}N simulation were given by:

$$\begin{aligned} &x_{\mathrm{N,VL}}(0) = \left(\frac{1}{\eta_{\mathrm{NC}}} - \frac{f_s}{\eta_{\mathrm{VS}}}\right) C_0, x_{\mathrm{N,VS}}(0) = \frac{f_s}{\eta_{\mathrm{VS}}} C_0, \\ &x_{\mathrm{N,MB}}(0) = x_{\mathrm{N,HL}}(0) = x_{\mathrm{N,HS}}(0) = 0 \end{aligned} \tag{9}$$

The function $f(x_{\mathrm{C,MB}}, x_{\mathrm{N,MB}})$ of Eq. (7) was defined in terms of $\eta_{\mathrm{MB}}^{\mathrm{lim}}$, the target value for the C : N ratio of the MB (η_{MB}). Two assumptions were tested:

1. an MB C : N ratio being constant throughout incubation:

$$f(x_{\mathrm{C,MB}}, x_{\mathrm{N,MB}}) = x_{\mathrm{N,MB}} - \frac{x_{\mathrm{C,MB}}}{\eta_{\mathrm{MB}}^{\mathrm{lim}}} \tag{10}$$

   For this function, there is only one parameter to be fitted for each site, $\eta_{\mathrm{MB}}^{\mathrm{lim}}$, all the other parameters being those fitted for ^{14}C simulations (Table 3).

2. an MB C : N ratio which fell linearly with incubation time from $\eta_{\mathrm{MB}}^{\mathrm{max}}$ to $\eta_{\mathrm{MB}}^{\mathrm{min}}$ at time t_c then constant at $\eta_{\mathrm{MB}}^{\mathrm{min}}$:

$$\begin{aligned} &f(x_{\mathrm{C,MB}}, x_{\mathrm{N,MB}}) = x_{\mathrm{N,MB}} - \frac{x_{\mathrm{C,MB}}}{\eta_{\mathrm{MB}}^{\mathrm{max}} - (\eta_{\mathrm{MB}}^{\mathrm{max}} - \eta_{\mathrm{MB}}^{\mathrm{min}})\frac{t}{t_c}} \text{ for } t \le t_c, \text{ otherwise} \\ &f(x_{\mathrm{C,MB}}, x_{\mathrm{N,MB}}) = x_{\mathrm{N,MB}} - \frac{x_{\mathrm{C,MB}}}{\eta_{\mathrm{MB}}^{\mathrm{inf}}} \text{ for } t > t_c \end{aligned} \tag{11}$$

   For this function three parameters must be fitted for each site: $\eta_{\mathrm{MB}}^{\mathrm{max}}$, $\eta_{\mathrm{MB}}^{\mathrm{min}}$ and t_c.

Two alternative simulation strategies were also tested: (a) simulated values of MB ^{15}N and inorganic ^{15}N were limited to positive values and (b) negative simulated values for MB ^{15}N and inorganic ^{15}N were allowed. The strategy (b) was used for the assumption 1 of a constant MB C : N ratio (although the model did not calculate many negative values, except at the start of simulation), both strategies were tested for the assumption 2 of a decreasing C : N ratio. Simulated negative values did not, of course, indicate that the ^{15}N content was really negative but that ^{14}N could replace ^{15}N to supply the nitrogen requirement.

For each incubation period, the model assumes that ${}^{15}_{\mathrm{inorg}}\dot{N}$, the inorganic ^{15}N remaining in the porous soil bags is the mineralized ^{15}N ($-\dot{N}$, Eq. 7) less the ^{15}N lost from the bag by plant uptake, leaching or gaseous losses, using a loss rate k_l:

$${}^{15}_{\mathrm{inorg}}\dot{N} = -\dot{N}(1 - k_l) \text{ if } {}^{15}_{\mathrm{inorg}}N > 0, \text{ otherwise } {}^{15}_{\mathrm{inorg}}\dot{N} = 0 \text{ if } {}^{15}_{\mathrm{inorg}}N \le 0 \tag{12}$$

The Powell optimization method was used to estimate the values of $\eta_{\mathrm{MB}}^{\mathrm{lim}}$, $\eta_{\mathrm{MB}}^{\mathrm{max}}$, $\eta_{\mathrm{MB}}^{\mathrm{min}}$, t_c, and k_l for the six experimental sites. The values of the other parameters (Table 3) remained unchanged from MOMOS-C calibration (Pansu et al., 2004) and validation (Pansu et al., 2010). The model was developed using VENSIM 5.6b (http://www.vensim.com).

2.4 Accuracy tests

The significance of the MOMOS simulations compared to the mean of measured values was tested by:

$$F = \frac{\sum_{i=1}^{n} (\bar{y}_i - \bar{y})^2 / (n-1)}{\sum_{i=1}^{n} (\bar{y}_i - \hat{y}_i)^2 / (n-p)} \tag{13}$$

where $i = 1, \ldots n$ is the number of sampling occasions ($n = 11$), p the number of model parameters which were specifically adjusted to predict the total production of inorganic ^{15}N ($p = 1$ for assumption 1, $p = 3$ for assumption 2), $\bar{y}_i$ the measured total remaining ^{15}N at i, $\hat{y}_i$ the corresponding MOMOS predicted value with assumption 1 or 2 and $\overline{y}$ is the mean of the data series for each site. A graphical representation (Figs. 2 to 7) shows whether the predicted values were within or outside the confidence intervals of the corresponding data series.

F tests were performed using RSS_T the residual sum of squares between the measured values and the values predicted by MOMOS for assumptions 1 and 2 (Table 4):

$$F_{y_{\mathrm{A12}}} = \frac{\mathrm{RSS}_{\mathrm{A1}}}{\mathrm{RSS}_{\mathrm{A2}}} = \frac{\sum_{i=1}^{n} (\bar{y}_i - \hat{y}_{i\mathrm{A1}})^2 / (n-1)}{\sum_{i=1}^{n} (\bar{y}_i - \hat{y}_{\mathrm{A2}})^2 / (n-3)} \tag{14}$$

where $\hat{y}_{\mathrm{A1}}$ and $\hat{y}_{i\mathrm{A2}}$ were the predicted values for assumptions 1 and 2, respectively. An F value (Eq. 11) greater than $F^{0.05}_{(n,n-p)}$ indicates that assumption 1 must be rejected at 5 % significance level: $\mathrm{RSS}_{\mathrm{A1}}$ was significantly greater than $\mathrm{RSS}_{\mathrm{A2}}$ and so assumption 1 predictions were significantly less accurate than assumption 2 predictions. A non significant F test (Eq. 14) meant the two assumptions did not give significantly different predictions.

3 Results

3.1 Mineralization of added ^{15}N

The model assumed that mineralized ^{15}N was the difference between added ^{15}N and the remaining ^{15}N. The largest part of this mineralized ^{15}N was exported from the porous soil bags by root absorption, water leaching or gaseous losses, since mineral ^{15}N remaining in bags represented only 1–3 % of the mineralized ^{15}N (Figs. 2–7). The data showed a decrease in ^{15}N mineralization rates from low altitude sites to higher sites. About 63 % of the added ^{15}N was mineralized at the lowest sites A(65) and A(165), 57 % at A(780), 47 % at A(1800), 25 % at A(3400) and 31 % at A(3968). The ^{14}C mineralization at the end of incubation (Pansu et al., 2010) was higher at about 80 % of the added ^{14}C at the lowest sites A(65) and A(165), 75–80 % at A(780) and A(1800) and 45 % at the highest sites A(3400) and A(3968), which indicated the same trend for both ^{14}C and ^{15}N, all values being well predicted by MOMOS.

3.2 Prediction using constant MB C : N ratio

The predicted values of ^{15}N mineralization (Table 4) using a constant MB C : N ratio during incubation, assumption 1 (Eq. 10) corresponded with the measured values only for low altitude sites at 1 % significance level for A(65) and A(165) and 5 % significance level for A(780). Predicted values were within the 95 % confidence interval of the measured data for A(165) (Fig. 3), slightly overestimated between 360 and 500 d incubation for A(65) (Fig. 2) and after 5 months incubation for A(780). For A(1800), the values were slightly underestimated for the first three months and 20 % overestimated after 8 months of incubation. This effect was larger for the two higher sites where the predicted values agreed with the measurements only for the first year of incubation, after 3 yr of incubation the overestimate was 35 % for A(3968) and 50 % for A(3400).

3.3 Prediction of ^{15}N mineralization using variable MB C : N ratio

Assumption 2 (Eq. 11) gave more accurate predictions than assumption 1, especially at high altitude. The predicted values of ^{15}N mineralization (Table 4) corresponded with the measured values at 1 % significance level for 5 of the 6 sites. For A(3400), the predicted values were not significantly close to the mean of the measurements. In five cases, the predicted values were significantly closer when assumption 2 was used, at 1 % significance level for A(65), A(780), and A(1800) and at 5 % significance level for A(3400) and A(3968). There was no significant difference for A(165). Using the strategy (b), which allowed negative values for inorganic ^{15}N and MB ^{15}N, gave closer predicted values for the two highest sites, at 1 % significance level for A(3968) and 5 % significance level for A(3400).

For A(65), A(780) and A(1800) (Figs. 2, 4, 5), the predicted values, using variable MB C : N ratio, truncating negative values (strategy (a)), were within the 95 % confidence intervals of all the measurements. For A(3400) (Fig. 6), 10 of the 11 predicted values were within the 95 % confidence intervals for both strategy (a) (curve 2) and strategy (b) (curve 3). For A(3968) (Fig. 7), 9 of the 11 predicted values were within the 95 % confidence intervals of the measurements when strategy (a) was used (curve 2). All predicted values were within the 95 % confidence intervals when strategy (b) was used (curve 3).

3.4 Prediction of other N labeled compartments

Unfortunately measurements were only available for the first five periods for MB ^{15}N and inorganic-^{15}N in the soil bags (see material and methods) and the model fit was not significant.

For A(65) (Fig. 2), 4 of the 5 MB ^{15}N values were slightly over-estimated using assumption 1 (curve 1) and 3 were overestimated using assumption 2 (curve 2). However, over the same period, the MB ^{14}C values were slightly underestimated. For A(165) (Fig. 3), MB ^{15}N values were overestimated while the MB ^{14}C predicted values were

always within the 95 % confidence intervals. For A(780) (Fig. 4), the last MB ^{15}N value was slightly underestimated (but within its wide confidence interval) while the 3 previous values were underestimated. However, over the same period, the MB ^{14}C values were underestimated. For A(1800) (Fig. 5), 3 values of MB ^{15}N were accurately predicted while one was underestimated and one was overestimated. For A(3400) (Fig. 6), both the MB ^{15}N and the MB ^{14}C values were overestimated. For A(3968) (Fig. 7), 2 of the 5 MB ^{15}N values were overestimated as were the last 6 MB-^{14}C values.

All predicted values for organic ^{15}N in the soil bags were close to the 95 % confidence intervals and sometimes closer with assumption 1 or assumption 2 but without any significant differences between the two assumptions.

In all cases, the model predicted a relatively large storage of ^{15}N in the labile microbial metabolites (HL compartment), which was about 80 % of the organic forms of ^{15}N at the end of experiment. NC ^{15}N was predicted as being almost exhausted and the rest of the ^{15}N was divided between microbial biomass (MB) and stable humus (HS) with a ^{15}N-MB : ^{15}N-HS ratio which increased with altitude (Figs. 2–7).

4 Discussion

4.1 Relationship between N and C cycles

These modeling results provide a positive answer to the first two questions raised in the introduction:

1 Can it be considered that microbial enzymatic assimilation rates are the same for C and N? Yes, we can argue that because all the parameters that had been defined for the MOMOS-C model, and their dependence on climate, quality of dead plant materials and soil texture, were retained for modeling the N cycle. This study shows that there is a strong link between the transfer processes of C and N from natural organic compounds.

2 Can it be considered that C transfers by microbial respiration and mortality cause simultaneous transfers of N into labile humus and inorganic forms to balance the MB C : N ratio? Yes, this modelling study demonstrates the simultaneous MB-N transfer into labile humus by microbial mortality and into inorganic N by ammonification. Moreover, can the assimilation of inorganic N be modelled to sustain microbial activity in the case of an N deficit during conversion of organic forms? Yes, an assimilation of inorganic N is modelled to sustain microbial activity in case of N deficit during the transformation processes.

This study also provided an answer to question 3: can it be considered that the microbial biomass is homeostatic or does it have a C : N ratio that varies through incubation periods and is different in ecosystems at different altitudes? The model predictions using the assumption of a constant MB C : N ratio over the incubation period gave MB C : N values (Table 4) ranging from 13.6 at the tropical savannah site A(165) to 22.8 at the highest site A(3968). These values were close to the measured total C : N ratios (Table 1) for the six sites, suggesting that the quality of living and dead organic materials converge to similar values after long fallow periods. They could appear high since the C : N ratio is generally allowed to vary within a restricted range between about 5 and 15 (Manzoni and Porporato, 2009). Other results could suggest higher values, e.g. Bottner et al. (2006) measured MB ^{14}C : ^{15}N ratios from 7.9 ± 1.3 for a substrate ^{14}C : ^{15}N ratio of 26.8 to 33.9 ± 7.5 for a substrate ^{14}C : ^{15}N ratio of 130 (2 × 10 measurements in two sites). As a first approximation for future applications of MOMOS, constant values could be used over the incubation period, especially for the low altitude sites.

Especially for the high altitude sites in this study, the predicted values were significantly more accurate when the MB C : N ratio was reduced linearly with the incubation time. With excess C at the start of incubation, the MB C : N ratio was the highest, which encouraged microbial immobilization of inorganic N. The C : N value was reduced linearly with time to its minimum value associated with a reduction in C mineralization, with a lower slope at higher altitudes. The minimum values found for MB C : N ratios (Table 4) were in the commonly accepted range, except at the high altitude site A(3968)

where CO_2-C respiration was reduced by lower temperatures. Bottner et al. (2006) showed that total respired CO_2-^{14}C was lower for nitrogen-poor straw than for nitrogen-rich straw, which was partly explained by an increase in microbial mortality (k_{MB} rate) which could increase the HL reserve which is richer in N than stable NC and can sustain MB and its conversions to inorganic N.

Except for A(165)and A(3968), the slopes of the MB C : N ratio vs. time decreased with increasing altitude (t_c in Table 4). This appears to be consistent with a decrease in metabolic rates with temperature (Eqs. 1 and 2).

Allowing negative values for inorganic ^{15}N (immobilization of inorganic ^{14}N) only significantly improved the predicted values for ^{15}N mineralization at the two high altitude sites, especially at the highest. For these sites, the model predicted microbial immobilization of N not only at the start of incubation but also later on during incubation. This strange behavior needs to be investigated by other experiments.

4.2 Ecological consistency and parsimony

This study established that there is a strong link between the C and N assimilation, the only difference between the model for C and the model for N being the modeling of the microbial conversions to and from inorganic compounds. Carbon is removed from the system as the CO_2 from microbial respiration (Eqs. 5 and 6), while inorganic N recycles rapidly in the soil in equilibrium with microbial N. This confirms that MB acts as a very active, short-term reserve, temporarily storing C and N, releasing C by respiration, producing C,N labile humus compounds (HL in Fig. 1), by mortality and exudation, recycling the major part of this HL and converting to and from mineral forms of N. The MOMOS model encompasses the principle of parallel C and N assimilation (see PAR models in the introduction) as it includes simultaneous, direct microbial assimilation of plant and humus compounds, ammonium production by microorganisms and, possibly, microbial assimilation of the ammonium produced. In terms of number and definition of its parameters, MOMOS is parsimonious (Ockham's razor), this model should fill a gap shown above in introduction for the modeling of “direct microbial control over decomposition”.

References

Barraclough, D.: The direct or MIT route for nitrogen immobilization: a ^{15}N mirror image study with leucine and glycine, Soil Biol. Biochem., 29, 101–108, 1997.

Bottner, P., Pansu, M., Sarmiento, L., Hervé, D., Callisaya-Bautista, R., and Metselaar, K.: Factors controlling decomposition of soil organic matter in fallow systems of the high tropical Andes: a field simulation approach using 14C and ^{15}N labelled plant material, Soil Biol. Biochem., 38, 2162–2177, doi:10.1016/j.soilbio.2006.01.029, 2006.

Bradbury, N. J., Witmore, A. P., Hart, P. B. S., and Jenkinson, D. S.: Modelling the fate of nitrogen in crop and soil in the years following application of ^{15}N-labelled fertilizer to winter wheat, J. Agr. Sci., 121, 363–379, 1993.

Brookes, P. C., Landman, A., Pruden, G., and Jenkinson, D. S.: Chloroform fumigation and the release of soil nitrogen : a rapid direct extraction method to measure microbial biomass nitrogen in soil, Soil Biol. Biochem., 17, 837–842, 1985.

Carter, M. R., Parton, W. J., Rowland, I. C., Schultz, J. E., and Steed, G. R.: Simulation of soil organic carbon and nitrogen changes in cereal and pasture systems of southern Australia, Aust. J. Soil Res., 31, 481–491, 1993.

Dou, Z. and Fox, R. H.: Using NCSWAP to simulate seasonal nitrogen dynamics in soil and corn, Plant Soil, 177, 235–247, 1995.

Franko, U.: Simulation of carbon and nitrogen dynamics in rural areas, Landbauforsch. Volk., 46, 114–120, 1996.

Garnier, P., Néel, C., Mary, B., and Lafolie, F.: Evaluation of a nitrogen transport and transformation model in a bare soil, Eur. J. Soil Sci., 52, 253–268, 2001.

Joergensen, R. G. and Mueller, T.: The fumigation-extraction method to estimate soil microbial biomass: Calibration of the k(EN) value, Soil Biol. Biochem., 28, 33–37, 1996.

Lin, B.-L., Sakoda, A., Shibasaki, R., Goto, N., and Suzuki, M.: Modelling a global biogeochemical nitrogen cycle in terrestrial ecosystems, Ecol. Model., 135, 89–110, 2000.

Manzoni, S. and Porporato, A.: Soil carbon and nitrogen mineralization: theory and models across scales, Soil Biol. Biochem., 41, 1355–1379, 2009.

Mueller, T., Magid, J., Jensen, L. S., Svendsen, H., and Nielsen, N. E.: Soil C and N turnover after incorporation of chopped maize, barley straw and blue grass in the field: evaluation of the DAISY soil-organic-matter submodel, Ecol. Model., 111, 1–15, 1998.

Neill, C. and Gignoux, J.: Soil organic matter decomposition driven by microbial growth: a simple model for a complex network of interactions, Soil Biol. Biochem., 38, 803–811, 2006.

Nicolardot, B., Recous, S., and Mary, B.: Simulation of C and N mineralisation during crop residue decomposition: a simple dynamic model based on the C : N ration of the residues, Plant Soil, 83, 83–103, 2001.

Pansu, M. and Gautheyrou, J.: Handbook of Soil Analysis – Mineralogical, Organic and Inorganic Methods, Springer, Berlin, Heidelberg, New York, 993 pp., 2006.

Pansu, M., Thuriès, L., Larré-Larrouy, M. C., and Bottner, P.: Predicting N transformations from organic inputs in soil in relation to incubation time and biochemical composition, Soil Biol. Biochem., 35, 353–363, 2003.

Pansu, M., Bottner, P., Sarmiento, L., and Metselaar, K.: Comparison of five soil organic matter decomposition models using data from a ^{14}C and ^{15}N labeling field experiment, Global Biogeochem. Cy., 18, GB4022, doi:10.1029/2004GB002230, 2004.

Pansu, M., Martineau, Y., and Saugier, B.: A modelling method to quantify in situ the input of carbon from roots and the resulting C turnover in soil, Plant Soil, 317, 103–120, doi:10.1007/s11104-008-9791-1, 2009.

Pansu, M., Sarmiento, L., Rujano, M. A., Ablan, M., Acevedo, D., and Bottner, P.: Modeling organic transformations by micro-organisms of soils in six contrasting ecosystems: validation of the MOMOS model, Global Biogeochem. Cy., 24, GB1008, doi:10.1029/2009GB003527, 2010.

Penning de Vries, F. W. T., Jansen, D. M., ten Berge, H. F. M., and Bakema, A.: Simulation of Ecophysiological Processes of Growth in Several Annual Crops, Pudoc, Wageningen, 271 pp., 1989.

Quemada, M. and Cabrera, M. L.: CERES-N model predictions of nitrogen mineralized from cover crop residues, Soil Sci. Soc. Am. J., 59, 1059–1065, 1995.

Richter, J. and Benbi, D. K.: Modeling of nitrogen transformations and translocations, Plant Soil, 181, 109–121, 1996.

Sterner, R. W. and Elser, J. J.: Ecological stoichimometry, in: The Biology of Elements from Molecules to Biosphere, edited by: Press, P. U., Princeton and Oxford, 2002.

Thuriès, L., Pansu, M., Larré-Larrouy, M. C., and Feller, C.: Biochemical composition and mineralization kinetics of organic inputs in a sandy soil, Soil Biol. Biochem., 34, 239–250, 2002.

Todd-Brown, K. E. O., Hopkins, F. M., Kivlin, S. N., Jennifer M. Talbot, J. M., and Allison, S. D.: A framework for representing microbial decomposition in coupled climate models, Biogeochemistry, 109, 19–33, doi:10.1007/s10533-011-9635-6, 2012.

Van Veen, J. A., Ladd, J. N., and Amato, M.: Turnover of carbon and nitrogen through the microbial biomass in a sandy loam and a clay soil incubated with [^{14}C(U)]glucose and [^{15}N](NH$_4$)$_2$SO$_4$ under different moisture regimes, Soil Biol. Biochem., 17, 747–756, 1985.

Table 1. Site characteristics.

Site Number	El Vigia A(65)	Barinas A(165)	Tovar A(780)	Merida A(1800)	Gavidia A(3400)	El Banco A(3968)
			Site characteristics			
Altitude m	65	165	780	1800	3450	3940
Latitude N	8°37′33″	8°36′55″	8°20′32″	8°37′39″	8°40′04″	8°48′52″
Longit. W	71°40′6″	70°12′15″	71°43′39″	71°9′17″	70°54′58″	70°55′30″
Typical ecosystem	Tropical rainforest	Natural savanna	Seasonal forest	Cloud forest	Andean páramo	High páramo
Actual vegetation	Managed grassland	Natural savanna	Managed grassland	Managed grassland	20 yr fallow	Natural páramo
Temperature[a]	27.4	26.4	23.0	17.4	8.9	5.5
Precipitation[b]	1825	1565	1112	1992	1338	790
AET[b]	1711	1297	1054	785	557	515
			Soil characteristics			
WRB type[c]	Inceptisol	Alfisol	Mollisol	Inceptisol	Inceptisol	Entisol
C g kg^{-1}	36.77	13.67	48.23	102.27	100.57	61.53
N g kg^{-1}	2.80	0.90	3.70	6.10	5.27	2.77
C : N	13.1	15.2	13.0	16.8	19.1	22.2
pH$_{\text{water}}$	5.1	5.7	6.1	5.2	4.6	4.7
CEC[d]	13.9	5.2	13.1	26.5	24.8	12.1
Sand (%DW)	67.3	77.0	62.0	69.3	40.0	62.0
Silt (%DW)	24.0	14.0	31.3	25.3	42.0	30.0
Clay (%DW)	8.7	9.0	6.7	5.3	18.0	8.0
WHC[e]	37.82	14.69	21.38	37.71	35.67	21.42
WCWP[e]	16.29	2.33	4.78	29.68	18.09	7.10
WCI[e]	27	8.5	13	33	26	14

[a] Long-term annual mean temperature in °C.

[b] Long-term annual mean precipitation and evapo-transpiration (mm).

[c] World Reference Basis.

[d] Cation Exchange Capacity mmol (+) kg^{-1}.

[e] Water Holding Capacity, Water Content at Wilting Point, and Initial Water Content in soil bags (% DW).

Table 2. Composition of soil in bags buried in 5–10 cm soil layer.

Site	g straw/ bag[a]	mg straw C/ bag[b]	mg straw N/ bag[c]	g soil + straw/bag[a]	mg N g^{-1} soil + straw[a]	% ^{15}N[a]	% ^{15}N excess[d]
A(65)	1.08	423.36	13.32	189.32	2.88	0.6094	0.2434
A(165)	1.08	423.36	13.32	225.43	0.93	0.8815	0.5155
A(780)	0.84	329.28	10.36	151.31	3.90	0.5347	0.1687
A(1800)	0.84	329.28	10.36	113.11	6.98	0.4964	0.1304
A(3400)	0.48	188.16	5.92	160.97	5.40	0.4310	0.0650
A(3968)	0.48	188.16	5.92	182.69	2.88	0.4857	0.1197

Straw C = 392 mg g^{-1}; straw N = 12.33 mg g^{-1}; straw C : N ratio = 31.79.

^{15}N natural abundance = 0.366 %.

[a] Measured values.

[b] g straw × straw C.

[c] g straw × straw N.

[d] %^{15}N – ^{15}N natural abundance.

Table 3. Parameter values used in the MOMOS-C model (Pansu et al., 2010) and retained in this N study.

Parameter	Definition	Units	Reference	Values A(65)	A(165)	A(780)	A(1800)	A(3400)	A(3968)
f_s	Stable C fraction of added NC	None	TAO model, Thuriès et al. (2002), Pansu and Thuriès (2002), Kaboré et al. (2010, 2011)	0.144					
k_{VL}	Microbial assimilation rate of labile NC	day^{-1}	$MAX(0.65 - 0.0019\eta_{NC}, 0.1)$ Bottner et al. (2006)	0.590					
k_{VS}	microbial assimilation rate of stable NC	day^{-1}	$MAX(0.0037 - 0.000026\eta_{NC}, 0.00005)$ Bottner et al. (2006)	0.0028					
k_{HL}	Microbial assimilation rate of labile humus	day^{-1}	0.05 Pansu et al. (2004)	0.05					
k_{HS}	Microbial assimilation rate of stable humus	day^{-1}	0.00005 Pansu et al. (2004)	0.00005					
k_{HLS}	Rate of stabilization of HL to HS	day^{-1}	0.0003 Pansu et al. (2004)	0.0003					
k_{MB}	Mortality rate of MB	day^{-1}	$MIN(0.42 + 0.0012\eta_{NC}, 0.8)$ Bottner et al. (2006)	0.458					
k_{resp}	Microbial respiration	day^{-1}	$-0.0008F_{0-20} + 0.062$ Pansu et al. (2007, 2010)	0.029	0.038	0.034	0.029	0.021	0.022
C_0^{BM}	MB-C at steady state	g MB – ^{14}C g^{-1} added-^{14}C	Pansu et al. (2010)	0.0107	0.0106	0.0192	0.0129	0.0185	0.0156

MB is microbial biomass, NC is added necromass, η_{NC} is the NC C : N ratio.

Table 4. Values and significance of additional parameters for MOMOS-N (this study).

Parameter	Definition	Units	Description	Values					
				A(65)	A(165)	A(780)	A(1800)	A(3400)	A(3968)
η_{MB}^{lim}	MB C : N ratio	None	Assumption 1 constant C : N ratio	18.3	13.6	19.3	18.9	19.1	22.8
F test	Eq. (13)		Assumption 1 constant C : N ratio	6.5[a]	9.2[a]	3.1[b]	1.6 NS	0.6 NS	0.7 NS
η_{MB}^{min}	Minimum value of MB C : N ratio	None	Assumption 2 variable C : N ratio	13.7	12.9	14.2	13.0	12.2	18.7
η_{MB}^{max}	Maximum value of MB-C : N ratio	None	Assumption 2 variable C : N ratio	23.5	33.7	24.0	23.7	21.4	42.8
t_c	Time for linear decrease from η_{MB}^{min} to η_{MB}^{max}	days	Assumption 2 variable C : N ratio	139	5	226	325	978	66
F test	Eq. (13)		Assumption 2 variable C : N ratio	68.6[a]	7.8[a]	32.9[a]	12.4[a]	2.3 NS	6.1[a]
$F_{y_{H12}}$ test	Eq. (14)		Assumption 2, negative values not possible	10.6[a]	0.8 NS	10.6[a]	7.7[a]	3.7[b]	3.6[b]
$F_{y_{H12}}$ test	Eq. (14)		Assumption 2, negative values possible					4.2[b]	9.2[a]
k_l	Rate of transfer of mineral ^{15}N to plants and losses	day^{-1}	Assumption 1 constant C : N ratio	0.65	0.14	0.24	0.25	0.17	0.48
k_l	Rate of transfer of mineral ^{15}N to plants and losses	day^{-1}	Assumption 2 variable C : N ratio	0.21	0.11	0.19	0.21	0.16	0.07

MB is the microbial biomass.

[a] 1 % significance level.

[b] 5 %, significance level.

NS not significant.

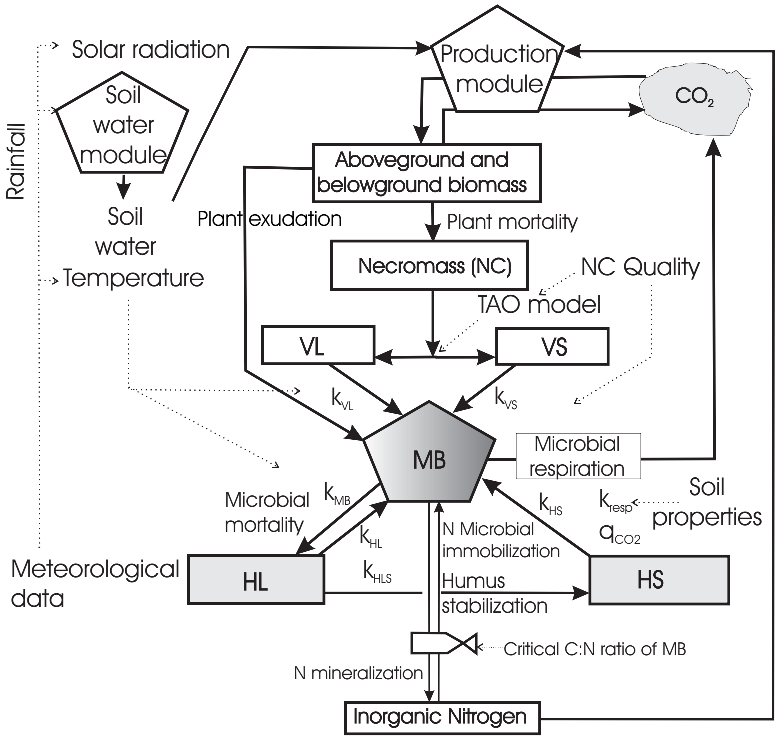

Fig. 1. Flow diagram for the MOMOS model coupled with a soil water module and a production module; MB is the microbial biomass, VL is the labile necromass (NC), VS is the stable necromass (NC); HL is the labile humus, HS is the stable humus; see Table 3 for meaning of the *k* parameters.

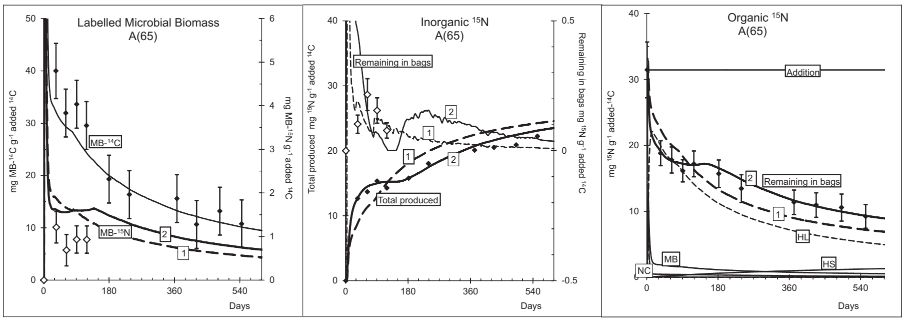

Fig. 2. Labeled microbial biomass (left), inorganic (centre) and organic forms (right) of ^{15}N in A(65), points are measurements with 95 % confidence intervals, lines are values predicted by the model using (1) assumption 1 (dashed lines) or (2) assumption 2 and strategy (a) (solid lines), MB is microbial biomass, HL is labile humus ^{15}N, HS is stable humus ^{15}N, NC is necromass ^{15}N.

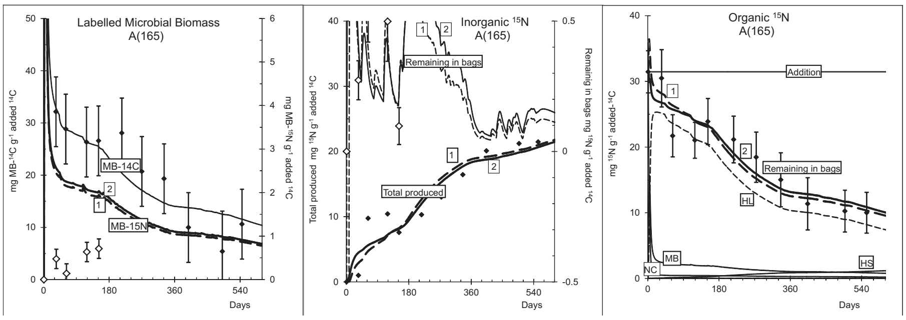

Fig. 3. Labeled microbial biomass (left), inorganic (centre) and organic forms (right) of ^{15}N in A(165), points are measurements with 95 % confidence intervals, lines are values predicted by the model using (1) assumption 1 (dashed lines) or (2) assumption 2 and strategy (a) (solid lines), MB is microbial biomass, HL is labile humus ^{15}N, HS is stable humus ^{15}N, NC is necromass ^{15}N.

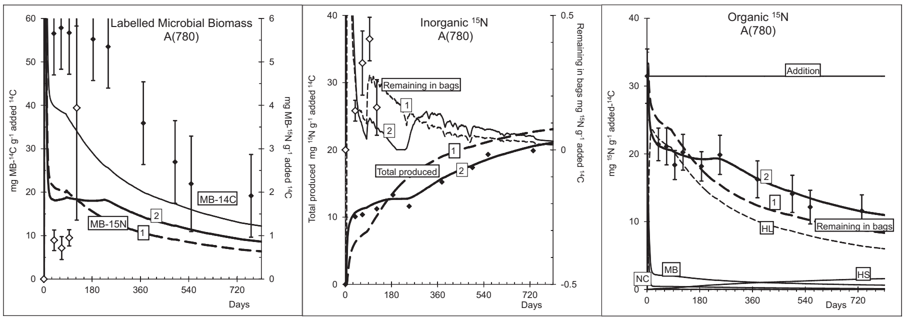

Fig. 4. Labeled microbial biomass (left), inorganic (centre) and organic forms (right) of ^{15}N in A(780), points are measurements data with 95 % confidence intervals, lines are values predicted by the model using (1) assumption 1 (dashed lines) or (2) assumption 2 and strategy (a) (solid lines), MB is microbial biomass, HL is labile humus ^{15}N, HS is stable humus ^{15}N, NC is necromass ^{15}N.

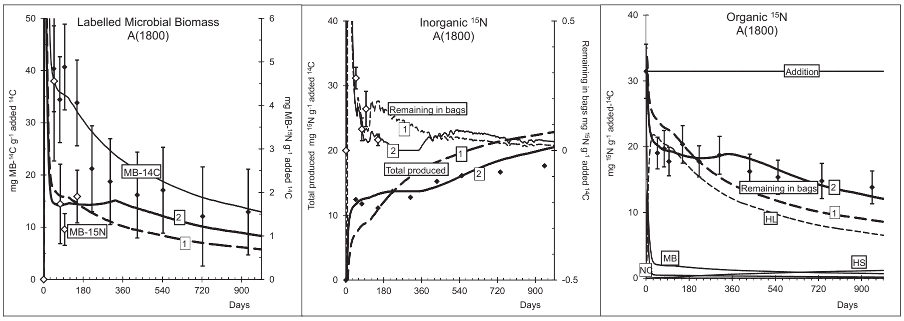

Fig. 5. Labeled microbial biomass (left), inorganic (centre) and organic forms (right) of ^{15}N in A(1800), points are measurements with 95 % confidence intervals, lines are values predicted by the model using (1) assumption 1 (dashed lines) or (2) assumption 2 and strategy (a) (solid lines), MB is microbial biomass, HL is labile humus ^{15}N, HS is stable humus ^{15}N, NC is necromass ^{15}N.

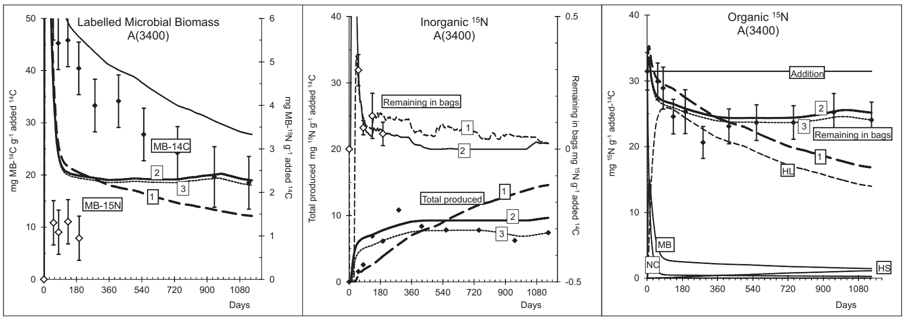

Fig. 6. Labeled microbial biomass (left), mineral (centre) and organic forms (right) of ^{15}N in A(3400), points are measurements with 95 % confidence intervals, lines are values predicted by the model using (1) assumption 1 (dashed lines), (2) assumption 2 and strategy (a) (solid lines), or (3) assumption 2 and strategy (b) (dashed lines) MB is microbial biomass, HL is labile humus ^{15}N, HS is stable humus ^{15}N, NC is necromass ^{15}N.

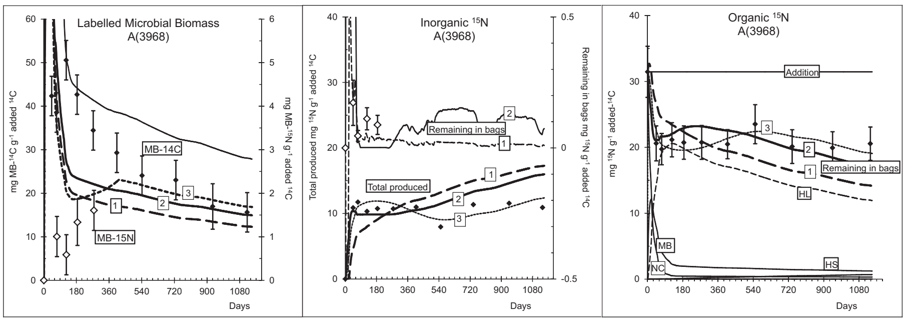

Fig. 7. Labeled microbial biomass (left), mineral (centre) and organic forms (right) of ^{15}N in A(3968), points are measurements with 95 % confidence intervals, lines are values predicted by the model using (1) assumption 1 (dashed lines), (2) assumption 2 and strategy (a) (solid lines), or (3) assumption 2 and strategy (b) (dashed lines) MB is microbial biomass, HL is labile humus ^{15}N, HS is stable humus ^{15}N, NC is necromass ^{15}N.